IOPscience iopscience.iop.org

Home Search Collections Journals About Contact us My IOPscience

Optical absorption and electron paramagnetic resonance of V^{4+} in GaP

This article has been downloaded from IOPscience. Please scroll down to see the full text article.

1998 J. Phys.: Condens. Matter 10 7619

(http://iopscience.iop.org/0953-8984/10/34/015)

View the table of contents for this issue, or go to the journal homepage for more

Download details:
IP Address: 171.66.16.209
The article was downloaded on 14/05/2010 at 16:42

Please note that terms and conditions apply.

J. Phys.: Condens. Matter **10** (1998) 7619–7632. Printed in the UK PII: S0953-8984(98)93555-X

Optical absorption and electron paramagnetic resonance of V^{4+} in GaP

W Ulrici†, K Friedland†, J Kreissl‡, A Erramli§, N Tebbal‖, A M Vasson‖¶ and A Vasson‖

† Paul-Drude-Institut für Festkörperelektronik, 10117 Berlin, Germany

‡ Heinrich-Hertz-Institut für Nachrichtentechnik Berlin GmbH, 10587 Berlin, Germany

§ LSM, Faculté des Sciences Semlalia, Université Cadi-Ayyad, BPS15, 40001 Marrakech, Morocco

‖ LASMEA, Université Blaise Pascal Clermont-Ferrand II, 63177 Aubiere, France

Received 22 June 1998

Abstract. The results of optical absorption, electrical conductivity, and electron paramagnetic resonance (EPR) experiments on different *p*-type GaP:V:Zn samples are reported. The $^2E \rightarrow {}^2T_2$ transition of V_{Ga}^{4+} gives rise to a broad triple-peaked absorption band and a zero-phonon line (ZPL) at 6968.3 cm^{-1}. These features are explained as due to a strong Jahn–Teller coupling of the $^2T_2$ state. The reduced spin–orbit splitting is smaller than the strain-broadened line-width (5 cm^{-1}) of the ZPL. The EPR spectrum of V_{Ga}^{4+}, which is angular dependent at $T < 4$ K, is analysed ($g = 1.960$, $A = 55.7 \times 10^{-4}$ cm^{-1}). Its intensity shows dependence on microwave power characteristics for an impurity with an ^2E ground state. The photo-induced recharging $V^{3+} \rightarrow V^{4+}$ is monitored by optical absorption as well as EPR and requires the recharging of P_{Ga} anti-site defects.

1. Introduction

In recent papers, the behaviour of vanadium as a substitutional impurity in GaP has been investigated by electrical, optical, electron paramagnetic resonance (EPR), and phonon scattering experiments [1–4]. The V_{Ga}^{2+}/V_{Ga}^{3+} acceptor level was found at $E_c - 0.58$ eV and several spectroscopic properties of V_{Ga}^{3+} could be clarified. The analysis of the photo-ionization transitions and photo-induced recharging processes of *n*-type SI-GaP:V suggested that the V^{3+}/V^{4+} donor level is located within the gap at about $E_v + (0.3 \pm 0.1)$ eV. Therefore, in *p*-type GaP:V, this level is expected to be partly or completely empty and besides V_{Ga}^{3+}, V_{Ga}^{4+} also becomes observable. $V^{4+}(d^1)$ in III–V semiconductors is of particular interest because it has the same very simple d^1 electron configuration as Ti_{Ga}^{3+}, which is well investigated in GaAs, GaP, and InP, but in contrast to the neutral Ti^{3+} it is positively charged. Therefore, from careful spectroscopic analyses of d^1 impurities in III–V semiconductors valuable information about transition metal impurities in III–V semiconductors can be expected, in particular about their electron–phonon interaction.

By capacitance spectroscopy (DLTS, DLOS) and optical absorption experiments on InP:V it has been verified that only the V_{In}^{3+}/V_{In}^{4+} donor level is located within the gap of InP at $E_v + 0.21$ eV [5, 6]. In *p*-type InP:V a zero-phonon line (ZPL) at 767.3 meV was detected in absorption and assigned to the $^2E \rightarrow {}^2T_2$ transition of V_{In}^{4+} [6].

¶ Deceased.

0953-8984/98/347619+14$19.50 © 1998 IOP Publishing Ltd

In the present paper we report on detailed optical absorption and EPR experiments on p-type GaP:V:Zn. The analysis of the spectra and the photo-induced recharging experiments allow the identification of the $^2E \rightarrow {}^2T_2$ absorption band associated with sharp lines of V^{4+}_{Ga} as well as the EPR signal due to V^{4+}_{Ga} in GaP; preliminary results of this had been published earlier [7]. This comprehensive investigation into the behaviour of V^{4+}_{Ga} in GaP also confirms the location of the V^{3+}_{Ga}/V^{4+}_{Ga} level within the gap at $E_v + 0.25$ eV as deduced from DLTS and DLOS experiments on the same samples [8].

2. Experimental details

The GaP boules investigated here were grown in the ⟨111⟩ direction by the liquid encapsulation Czochralski (LEC)-technique using a high-pressure puller. They had a diameter of 40 mm and length of about 100 mm. B_2O_3 was used as a liquid encapsulant. The boules were doped by the addition of metallic vanadium to the melt (1.2 mg V per g GaP) and of Zn_3As_2 to achieve p-type material. Two boules were grown (PI 1391 and PI 1535) with different Zn content (see table 1). The samples for all experiments were taken from the same slice (A1 or E1), which are cut to a thickness of 6 mm either from the seed end (A1, $g \approx 0.05$) or the tail end (E1, $g \approx 0.95$)† of the boules.

Table 1. Hole concentration p and Hall-mobility μ_H measured at $T = 300$ K on the investigated p-type GaP:V:Zn samples. E_a are the activation energies derived from the temperature dependence $\rho \cdot T^{3/2} = f(1/T)$ measured in the dark. The contents of vanadium ([V]) and zinc ([Zn]) in the samples are taken from spectrochemical analyses.

Sample	p (10^{16} cm^{-3})	μ_H (cm^2 V^{-1} s^{-1})	E_a (meV)	[V] (10^{16} cm^{-3})	[Zn] (10^{16} cm^{-3})
PI 1535-A1	0.46	48	155	0.9	6.1
PI 1535-E1	7.00	65	55	4.8	27.2
PI 1391-E1	0.37	74	160	5.3	4.8

The rectangular samples for the optical absorption experiments were polished to optical quality on all sides, the absorbing thickness varied from 1 to 15 mm. The samples were mounted in a cold-finger cryostat with LiF windows or in a continuous-flow cryostat (Oxford Instruments CF 1204). For the investigation of photo-induced recharging processes, i.e. the measurement of optical absorption during illumination perpendicular to the measurement beam, a tungsten halogen lamp (150 W) combined with metal interference filters as well as Si and GaAs edge filters was used. Optical absorption was measured with a double-beam prism spectrometer and with a Bruker IFS120 Fourier transform spectrometer equipped with CaF_2 beam splitter and cooled InSb detector.

For measuring the temperature-dependent Hall (TDH) effect, samples with dimensions of $7 \times 3 \times 0.5$ mm^3 with ohmic Au–Be contacts were used in a standard Hall configuration.

The EPR measurements were carried out on oriented samples $10 \times 3 \times 3$ mm^3 with long axis parallel to ⟨110⟩ using an X-band spectrometer Bruker ESP 300E. The 3×10 mm^2 faces of the samples are polished to permit photo-EPR experiments.

On the same samples the analogous experiments have been performed by thermally detected (TD)-optical absorption (OA) and TD-EPR. The equipments for TD-OA and TD-EPR (used in the X-band and Q-band) as well as the advantages of thermal detection have been described in detail elsewhere [9, 10].

† g is the fraction of melt solidified at a certain distance from the seed.

3. Results

3.1. Electrical measurements

The hole concentration p and the Hall-mobility μ_H derived from conductivity and Hall-effect measurements at $T = 300$ K are given in table 1 together with the contents of V and Zn determined spectrochemically. Figure 1 shows the temperature dependence of the resistivity measured on sample PI 1535-A1 between 300 K and 80 K in the dark as well as during illumination. The activation energies E_a taken from the slope of $\rho \cdot T^{3/2} = f(1/T)$ plots of figure 1 are also given in table 1. The p-conductivity of sample PI 1535-E1 is not affected by illumination and the measured $E_a = 55$ meV indicates that the Fermi-level E_F in this sample is pinned by the shallow Zn-acceptors [11, 12]. On the other hand, the resistivity in the dark of samples PI 1535-A1 and PI 1391-E1 increases strongly with decreasing temperature suggesting that E_F is located above the Zn-level. Assuming the Zn-acceptor level at $E_v + 70$ meV and the V-donor level at $E_v + 250$ meV as well as their contents given in table 1, the data points can reasonably fitted using the formulae given by Look [13, 14]. During illumination with the light-emitting diode ($h\nu_{max} \approx 1.9$ eV), the p-conductivity of sample PI 1535-A1 is drastically enhanced and determined by the Zn-acceptors as can be seen from the temperature dependence in figure 1 and the derived E_a. The conductivity of sample PI 1391-E1 is only slightly enhanced during illumination as it is expected from the larger [V]/[Zn] ratio of this sample compared with that of PI 1535-A1.

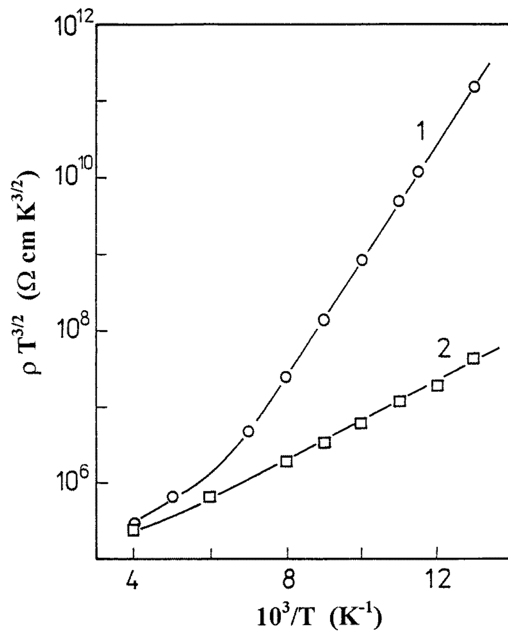

Figure 1. Temperature dependence of the resistivity of the GaP:V:Zn sample PI 1535-A1. Curve 1, in the dark (○); curve 2, during illumination with $h\nu \approx 1.9$ eV (□).

3.2. Optical absorption

Figure 2 shows the optical absorption spectra of the p-conducting sample PI 1535-E1. The spectra are dominated by intense absorption in the low-energy region due to the free holes and a strong photo-ionization absorption for $E > 1.2$ eV. In the spectrum at $T = 78$ K

(curve 2) a triple-peaked absorption band can be seen with the peak positions at 7400 cm^{-1}, 8200 cm^{-1}, and 8600 cm^{-1}. At higher temperatures ($T \approx 260$ K) two additional peaks appear on the high-energy side of the triple-peaked band. For a better analysis, figure 3 shows the absorption spectra after subtracting the intense absorptions seen in figure 2. For lower temperatures ($T = 7$ K), at the low-energy side of the triple-peaked band, two sharp lines at 6968.3 cm^{-1} and 6991.3 cm^{-1} with half-widths $\Gamma = 5$ cm^{-1} and 12 cm^{-1}, respectively, are measured (see figure 4). As this sample is *p*-conducting (see table 1), all V impurities are expected to be in the V^{4+} charge state at least at low temperatures. Therefore, we assign the triple-peaked band connected with the two sharp lines to the $^2E \rightarrow {}^2T_2$ transition of V^{4+}_{Ga}.

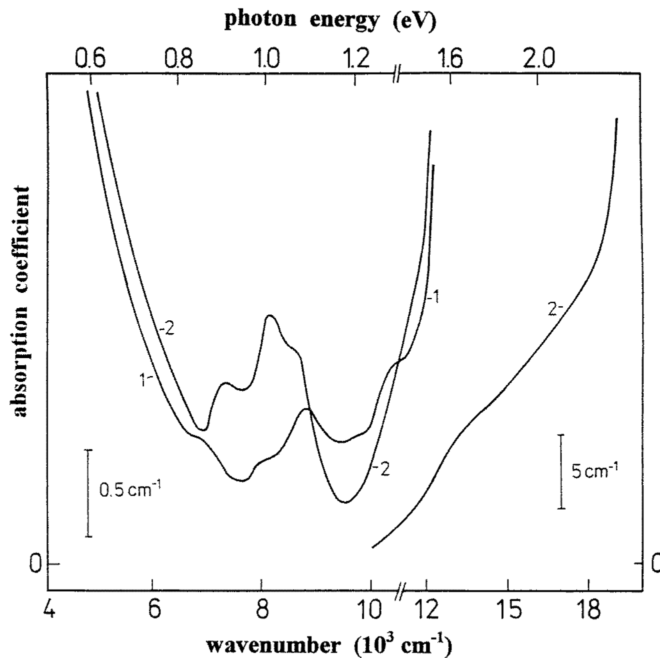

Figure 2. Optical absorption spectra of *p*-conducting GaP:V:Zn (sample PI 1535-E1). Curve 1, $T = 300$ K; curve 2, $T = 78$ K.

The additional bands appearing at temperatures $T > 260$ K can be identified as the components of the triple-peaked absorption band due to the $^3A_2 \rightarrow {}^3T_1(F)$ transition of V^{3+}_{Ga}. As the line shape of this V^{3+}_{Ga} band at different temperatures is known from previous investigations [3]†, a decomposition of the spectrum into the contribution arising from V^{3+}_{Ga} and V^{4+}_{Ga} can be carried out as it is shown for $T = 300$ K in figure 3. Such a decomposition was made for the spectra at different temperatures above 260 K and gave the following results.

(i) The line shape of the triple-peaked $^2E \rightarrow {}^2T_2$ band of V^{4+}_{Ga} and its temperature dependence indicate a strong $T \otimes \tau_2$ Jahn–Teller coupling of the excited $^2T_2$ state as the distances ΔE_H and ΔE_L between the central peak and the side peaks increase proportional to $[\coth(h\omega_\tau/2kT)]^{1/2}$. The analysis, which is analogous to the one described in [3] for the

† It is noted that erroneously figure 8 in [3] shows the absorption spectrum of a *p*-conducting GaP:V sample and the weak triple-peaked band seen there is the V^{4+}_{Ga} band discussed here.

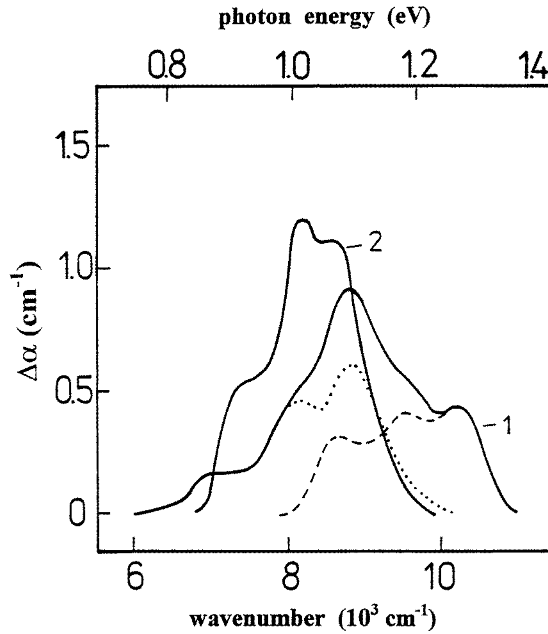

Figure 3. Optical absorption spectra of figure 2 after subtracting the intense absorption. Spectrum 1 ($T = 300$ K) is decomposed into the band due to the $^3A_2 \rightarrow {}^3T_1(F)$ transition of V^{3+}_{Ga} (dashed curve) and the band due to the $^2E \rightarrow {}^2T_2$ transition of V^{4+}_{Ga} (dotted curve). Spectrum 2, $T = 78$ K.

strongly τ_2-coupled $T_1(F)$ state of V^{3+}_{Ga} in GaP (see equation (1) and (2) in that paper), gives $\Delta E_H(0) = \Delta E_L(0) = 400$ cm^{-1}, $\Delta E_1 \approx 400$ cm^{-1}, $h\omega_\tau \approx 100$ cm^{-1}, and the Jahn–Teller energy $E_{JT} = (1000 \pm 200)$ cm^{-1}.

(ii) Using the areas under the V^{3+}_{Ga} and V^{4+}_{Ga} absorption bands, the temperature dependence of the $[V^{3+}]/[V]$ ratio can be obtained between 260 K and 360 K. The $\ln([V^{3+}]/[V]) = f(1/T)$ plot gives a straight line with an activation energy of $E_a = (160 \pm 40)$ meV. This result indicates a thermal population of the V^{3+}_{Ga}/V^{4+}_{Ga} level within the gap for temperatures above 260 K.

Curve 1 of figure 5 shows the absorption spectrum of sample PI 1535-A1 at $T = 300$ K. The triple-peaked band centred at about 1.2 eV is due to the $^3A_2 \rightarrow {}^3T_1(F)$ transition of V^{3+}_{Ga} and at low energies the weak free hole absorption can be seen (cf table 1). Curve 2 is the spectrum after cooling to $T = 78$ K in the dark. The free hole absorption has vanished (cf figure 1) and both the V^{3+}_{Ga} and V^{4+}_{Ga} bands can be seen. These bands are superimposed by a broad photo-ionization absorption with its onset at less than 0.4 eV and a second one with an onset at about 1.2–1.3 eV.

In figure 6, the absorption spectra at $T = 78$ K of sample PI 1391-E1 are shown. Again, both the V^{4+} and the V^{3+} band are detected but most of the V atoms are in the V^{3+} state. Compared with sample PI 1535-A1, this result is comprehensible as the Zn-content is nearly the same but the V-content is larger by a factor of about 5 (see table 1). At $T = 7$ K, the sharp lines connected with the V^{4+}_{Ga} band (cf figure 4) are measured as well as those belonging to the $^3A_2 \rightarrow {}^3T_2$ and $^3A_2 \rightarrow {}^3T_1(F)$ transitions of V^{3+}_{Ga} as can be seen in figure 7.

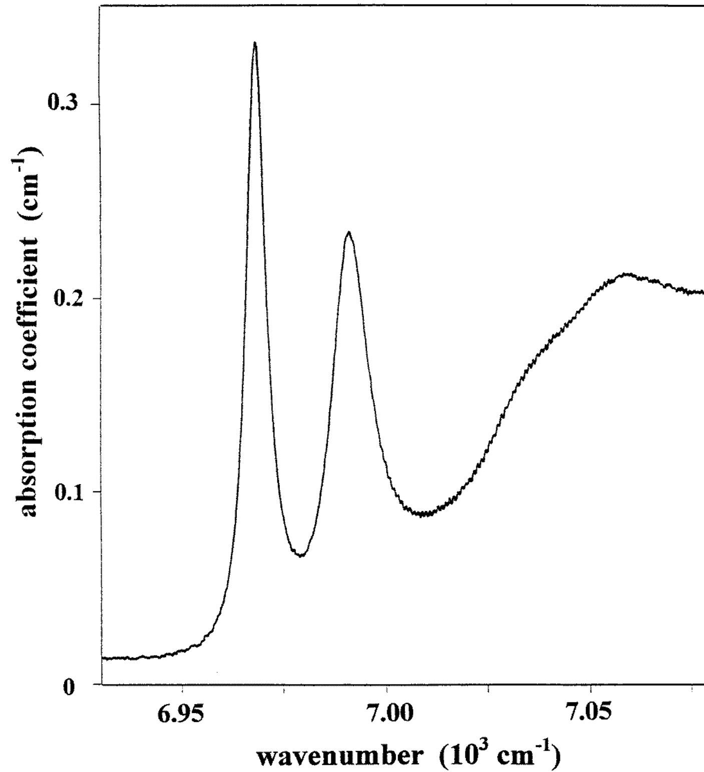

Figure 4. Sharp line absorption spectrum measured with high resolution at $T = 7$ K on sample PI 1535-E1 (cf figures 2 and 3).

3.3. Electron paramagnetic resonance

EPR measurements at $T = 20$ K on p-conducting samples (PI 1535-E1), which contain all V atoms in the V^{4+} state, reveal a broad isotropic signal shown in curve 1 of figure 8. The additional superimposed signal is the central line of the well known five-line spectrum due to Fe^{3+}_{Ga} (residual Fe impurity). Figure 9 shows this signal measured by TD-EPR at 35 GHz. The peak-to-peak intensity I^*_{pp} of the broad isotropic signal increases with increasing microwave power as $P^{1/2}$ and it was not saturable up to $P = 50$ mW at $T = 20$ K as shown in figure 10. This behaviour indicates a very short spin-lattice relaxation time as expected for a ^{2}E ground state suggesting that the signal is indeed due to V^{4+}_{Ga}. For comparison figure 10 also shows the dependence of the V^{3+}_{Ga} signal ($^3A_2$ ground state) on P [2], which saturates for P as low as 50 μW at $T = 20$ K. The isotropic V^{4+}_{Ga} signal can be analysed using the spin Hamiltonian $\mathcal{H} = g\mu \boldsymbol{SB} + A\boldsymbol{IS}$ with $S = 1/2$ and $I = 7/2$ (100% natural abundance of ^{51}V). The eight hyperfine (hf) lines (distance A, see figure 8) are not resolved because of the large line-width of each of the hf lines due to interaction of the d-electron with the nuclear spins of numerous of the surrounding P and Ga atoms. However, a computer simulation of the measured signal shape (curve 2 in figure 8) has delivered the parameters $g = 1.960 \pm 0.003$, $|A| = 55.7 \pm 0.7 \times 10^{-4}$ cm^{-1} and the width of each hf line $\Delta B_{pp} = 21$ mT.

At $T < 4.2$ K, the line intensity I^*_{pp} of the V^{4+}_{Ga} EPR line found to be angular dependent, a similar angular dependence is found for ΔB_{pp}. These angular dependences have been

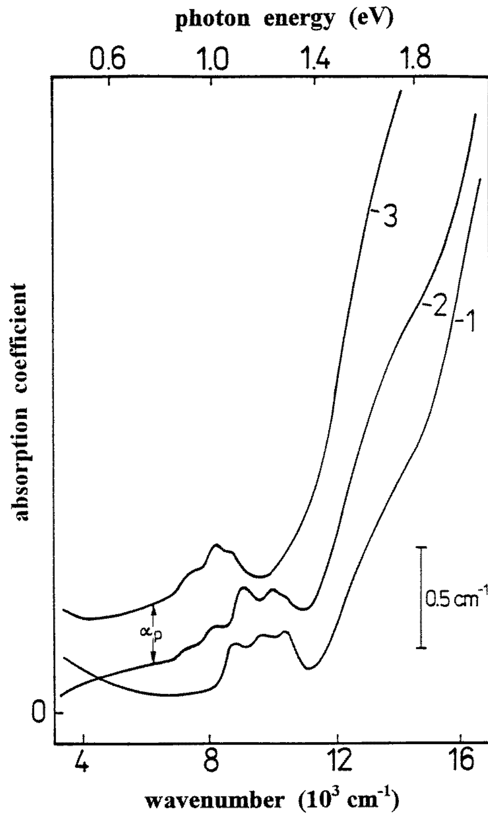

Figure 5. Optical absorption spectra of p-type GaP:V:Zn (sample PI 1535-A1). Curve 1, T = 300 K; curve 2, T = 78 K, after cooling in the dark; curve 3, T = 78 K during illumination with light of $h\nu_{exc} = 1.6$ eV.

investigated and interpreted in detail in [15] as a consequence of the simultaneous action of the vibronic $E \otimes \varepsilon$ Jahn–Teller coupling and of random strains on the ^{2}E ground state of V_{Ga}^{4+} according to the theoretical predictions of Ham [16]. The derived parameters of the corresponding Hamiltonian for a vibronic ^{2}E state are given in [15] together with those obtained for the isoelectronic d^1 system GaP:Ti^{3+}.

The EPR spectrum measured on sample PI 1535-A1 after cooling in the dark consists of a single broad signal, too. However, its dependence on microwave power P reveals two different components as can be seen from figure 11. This behaviour can be explained if we consider that the g-values of V_{Ga}^{4+} (1.960) and V_{Ga}^{3+} (1.963) are virtually identical as well as the hyperfine splittings A and that the V_{Ga}^{3+} signal saturates at low P (about 1 μW at $T = 1.5$ K and 50 μW at $T = 20$ K, cf figure 10). The EPR signal measured on this sample is a superposition of both the V_{Ga}^{3+} and V_{Ga}^{4+} signal. At low P, the signal is mainly due to V_{Ga}^{3+}. With increasing P this contribution saturates whereas the intensity of the V_{Ga}^{4+} signal increases as $P^{1/2}$. Finally, at high P the signal is mainly due to V_{Ga}^{4+}. This interpretation is confirmed by the result that, at $T = 1.5$ K, the signal measured at very low P is isotropic (as known for V_{Ga}^{3+}) whereas, at high P, it exhibits the angular dependence characteristic for V_{Ga}^{4+}. From figure 11 it can be seen that, at $T = 1.5$ K, the V^{4+} signal shows no saturation up to $P = 100$ mW, whereas for Ti^{3+} the saturation starts at $\approx$10 mW (see figure 10 in

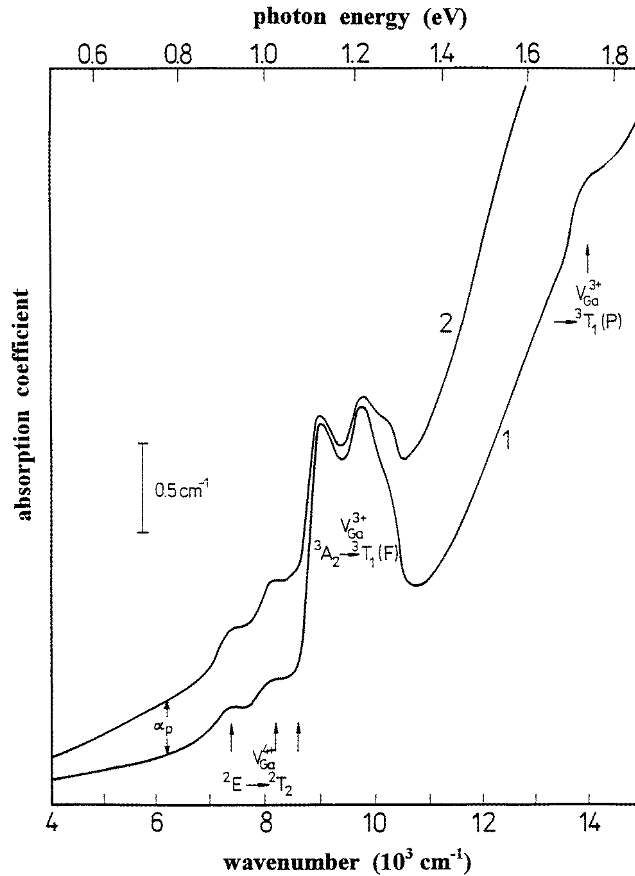

Figure 6. Optical absorption spectra of p-type GaP:V:Zn (sample PI 1391-E1) measured at $T = 78$ K. Curve 1, after cooling in the dark; curve 2, during illumination with light of $h\nu_{exc} = 1.6$ eV.

[15]). This indicates a stronger coupling of the ^{2}E ground state of V^{4+} to lattice vibrations compared with Ti^{3+}.

3.4. Photo-induced effects

On p-conducting samples PI 1535-E1 no changes could be observed in the optical absorption and EPR spectra during illumination with light in the energy region 0.5 eV $< h\nu_{exc} <$ 2.3 eV. On the other hand, the spectra of samples containing both V_{Ga}^{3+} and V_{Ga}^{4+} (PI 1535-A1, PI 1391-E1), i.e. with the Fermi level pinned by the V_{Ga}^{3+}/V_{Ga}^{4+} level at low temperatures, are considerably affected by illumination with such sub-band-gap light at $T < 120$ K. The changes found in optical absorption and EPR (both conventional and thermally detected) can be summarized as follows.

Curve 3 in figure 5 and curve 2 in figure 6 show the optical absorption spectra at $T = 78$ K during illumination with $h\nu_{exc} = 1.6$ eV. On sample PI 1535-A1, this illumination affects the disappearance of the V_{Ga}^{3+} band and the proportionate increase of the V_{Ga}^{4+} band as well as the proportionate enhancement of the broad photo-ionization absorption with onset

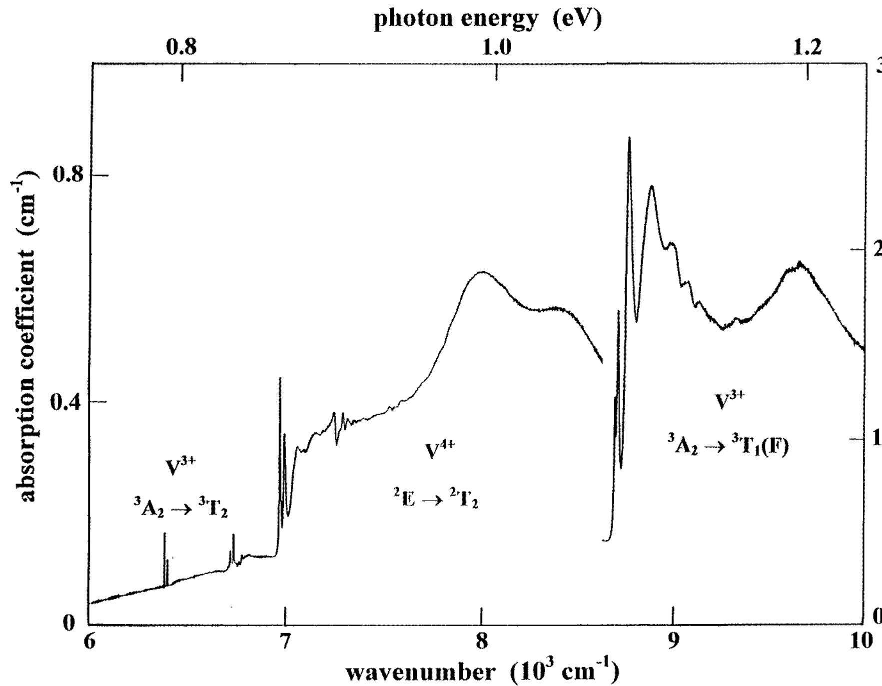

Figure 7. Optical absorption spectrum of sample PI 1391-E1 measured at $T = 7$ K.

at less than 0.4 eV. In order to have a measure for the change of this photo-ionization absorption which is proportional to the intensity of the V_{Ga}^{4+} band, its absorption coefficient $\alpha_p(0.77\ \mathrm{eV})$ is used (see figures 5 and 6). The sharp lines of the $^2E \rightarrow {}^2T_2$ transition of V_{Ga}^{4+} measured at $T = 7$ K (cf figure 4) are increased in intensity by the same factor as the broad V_{Ga}^{4+} band (figure 3) whereas the sharp lines due to the $^3A_2 \rightarrow {}^3T_1(F)$ transition of V_{Ga}^{3+} (cf figure 7) are strongly decreased. These results clearly indicate a nearly complete photo-induced recharging. This is confirmed by the EPR experiments. The dependence on microwave power P (cf figure 11) at $T = 1.5$ K after illumination with $h\nu_{exc} = 2.0$ eV shows that V_{Ga}^{3+} was no longer detectable and the V_{Ga}^{4+} signal intensity was enhanced. This vanishing of the V_{Ga}^{3+} signal is accompanied by the appearance of the phosphorous anti-site (P_{Ga}^{4+}) EPR signal.

On sample PI 1391-E1, the same photo-induced features are observed in optical absorption and EPR. However, in this sample the $V^{3+} \rightarrow V^{4+}$ recharging can be achieved only partly as can be seen from the remaining V_{Ga}^{3+} absorption band (figure 6) as well as the V_{Ga}^{3+} EPR signal. Further increases of the illumination intensity do not increase the V^{4+}/V^{3+} ratio.

The dependence of the photo-induced effects on the illumination energy $h\nu_{exc}$ has been monitored by optical absorption and EPR and the results for both samples are shown in figures 12 and 13. It can be seen that, onsetting at $h\nu_{exc} \approx 1.25$ eV, the spectral dependence of the following changes is nearly identical:

(i) the increase of α_p, i.e. the content of V_{Ga}^{4+};
(ii) the increase of the V_{Ga}^{4+} EPR signal;
(iii) the decrease of the $^3A_2 \rightarrow {}^3T_1(F)$ band of V_{Ga}^{3+};
(iv) the decrease of the V_{Ga}^{3+} EPR signal.

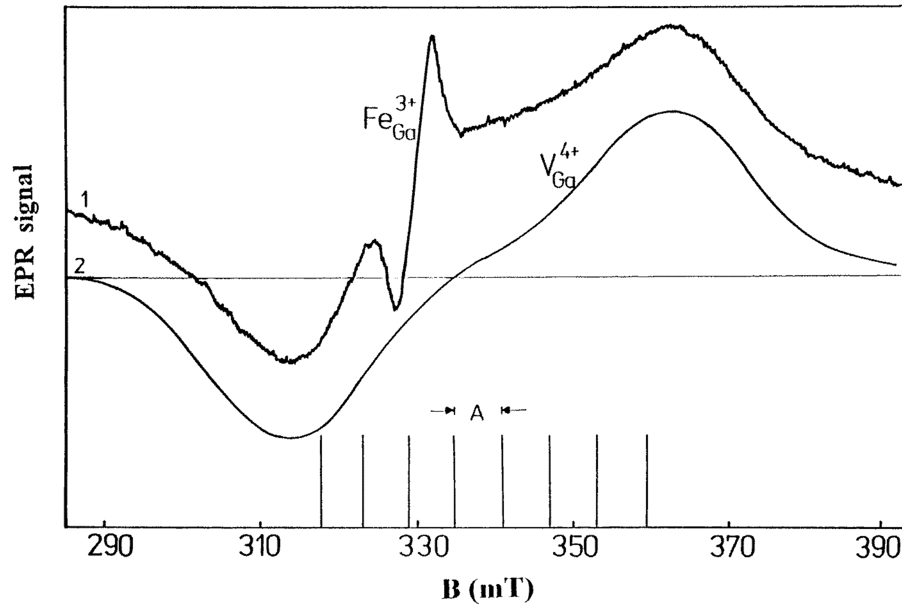

Figure 8. Curve 1, EPR-spectrum measured at $T = 20$ K on a p-conducting GaP:V:Zn sample (PI 1535-E1) with $\nu = 9.6$ GHz and $P = 40$ mW. Curve 2, simulated spectrum of curve 1 due to V^{4+}_{Ga} with the parameters g, A, and ΔB_{pp} given in the text. The stick spectrum at the bottom shows the unresolved splitting into eight lines due to hyperfine interaction with the ^{51}V nucleus ($I = 7/2$).

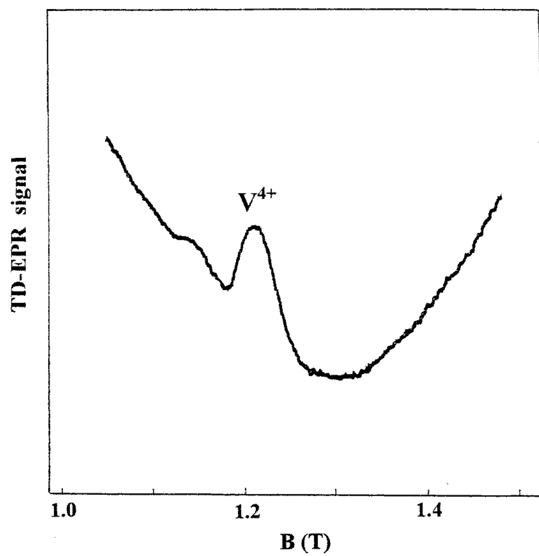

Figure 9. TD-EPR spectrum of sample PI 1535-A1 measured at $T = 5$ K and the microwave frequency $\nu = 34.85$ GHz.

The intensity of the Fe^{3+}_{Ga} EPR signal is not affected by $h\nu_{exc}$, i.e. the empty $Fe^{2+}_{Ga}/Fe^{3+}_{Ga}$ level at $E_v + 0.86$ eV is not involved in the recharging processes concerning V_{Ga}.

In both samples, the photo-induced rechargings reverse slowly in the dark after switching off the illumination. Monitoring the decay of α_p in the dark at $T = 78$ K the dependence

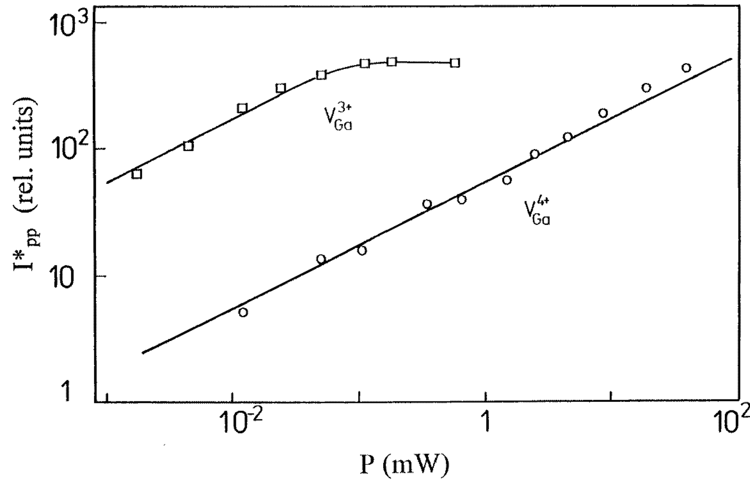

Figure 10. Dependence of the intensity I^*_{pp} of the V^{4+}_{Ga} EPR signal (cf figure 8) and of the V^{3+}_{Ga} EPR signal [2] on microwave power P measured at $T = 20$ K.

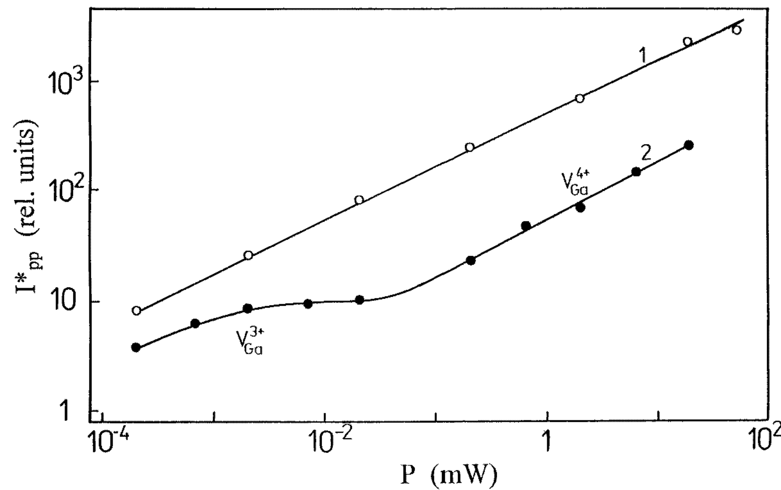

Figure 11. Dependence of the EPR signal intensity I^*_{pp} on the microwave power P measured at $T = 1.5$ K with $B \parallel \langle 111 \rangle$. Curve 1, sample PI 1535-E1 containing only V^{4+}_{Ga}. Curve 2, sample PI 1535-A1 after cooling in the dark, containing V^{4+}_{Ga} and V^{3+}_{Ga}.

$\alpha_p(t)/\alpha_p(0) \sim \ln(t/\tau)$ with $\tau \approx 2 \times 10^6$ s was found. Such a logarithmic decay was already investigated earlier for other photo-induced recharging processes including transition metal impurities in III–V semiconductors [17]. The photo-induced hole conductivity (see figure 1) decays in the dark in a similar way. However, the photo-induced $V^{3+} \rightarrow V^{4+}$ recharging cannot be reversed optically (in contrast to, e.g., the $V^{3+} \rightarrow V^{2+}$ process in GaP:V [3]), i.e. illumination with 0.4 eV $< h\nu_b <$ 1.1 eV does not accelerate the decay. To restore the original state, the samples have to be warmed up to about 170 K. The $V^{3+} \rightarrow V^{4+}$ recharging is in both samples also accompanied by an increase of the photo-ionization absorption at energies >1.2 eV.

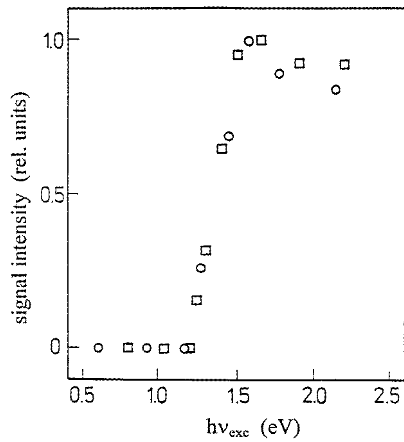

Figure 12. Dependence of the photo-induced changes on illumination energy $h\nu_{exc}$ measured on sample PI 1535-A1. Open circles, photo-induced absorption $\alpha_p(0.77$ eV) measured at $T = 78$ K; open squares, V_{Ga}^{4+} EPR signal measured at $T = 20$ K. The data points are normalized to the highest achieved one for both signals.

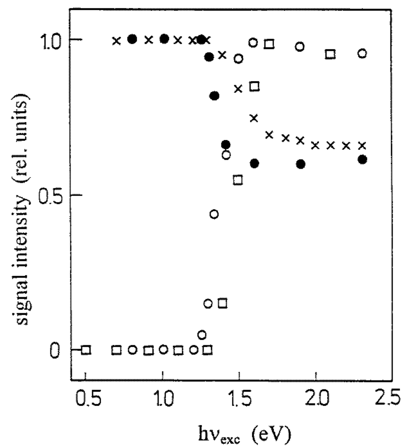

Figure 13. Dependence of the photo-induced changes on illumination energy $h\nu_{exc}$ on sample PI 1391-E1. Open circles and squares as in figure 12; full circles, $^3A_2 \rightarrow {}^3T_1(F)$ absorption band of V_{Ga}^{3+} measured at $T = 78$ K; crosses, V_{Ga}^{3+} EPR signal measured at $T = 20$ K. These two sets of data points are normalized to their dark values.

4. Discussion

4.1. The $^2E \rightarrow {}^2T_2$ transition of V_{Ga}^{4+}

The optical absorption experiments presented in section 3 clearly demonstrate that the $^2E \rightarrow {}^2T_2$ transition of V^{4+} is responsible for the broad triple-peaked absorption band accompanied by two sharp lines with a distance of 23 cm^{-1}. These lines were explained [7] as due to the zero-phonon lines (ZPL) of the $^2E(\Gamma_8) \rightarrow {}^2T_2(\Gamma_8)$ and $\rightarrow {}^2T_2(\Gamma_7)$ transitions (crystal field splitting 10 $Dq = 6970$ cm^{-1}) and their distance as due to the Jahn–Teller reduced spin–orbit splitting of the $^2T_2$ state. This interpretation followed that given for

the two sharp lines separated also by about 25 cm^{-1} measured in the absorption spectra of Ti^{3+} in GaP, GaAs, and InP. However, it was mentioned already in [7] that the Jahn–Teller coupling strength S_τ estimated with this interpretation is smaller by an order of magnitude compared with that derived from the temperature dependence of the triple-peaked absorption band ($S_\tau = E_{JT}/h\omega_\tau \approx 10$ for V^{4+}, i.e. strong coupling, see section 3.1).

In the meantime, detailed investigations have been carried out on the $^2E \to {}^2T_2$ transition of the isoelectronic Ti^{3+}_{Ga} in GaP [18]. The splitting of the ZPLs of GaP:Ti^{3+} under uniaxial stress has unequivocally verified that the spin–orbit splitting of the excited $^2T_2$ state into the Γ_7 and Γ_8 states amounts to only 3.3 cm^{-1}. The theoretical analysis of the stress splittings, which required to take into account the Jahn–Teller coupling of the $^2T_2$ state with both τ_2- and ε-modes up to second order, has shown that it is indeed a strong Jahn–Teller coupling.

The V^{4+}_{Ga} impurity (positively charged) attracts the ligand electrons stronger than the isoelectronic Ti^{3+}_{Ga} (neutral), i.e. there is a stronger overlap of the d-orbitals with the p-orbitals of the surrounding phosphorous ligands. This larger overlap results in a stronger coupling to the lattice vibrations and a stronger sensitivity to lattice strains for V^{4+} compared with Ti^{3+}. The half-width of the individual ZPLs of GaP:Ti^{3+} are $\Gamma \approx 0.5$ cm^{-1} at $T = 7$ K [18] whereas a value of $\Gamma = 5$ cm^{-1} was found for the first sharp line of GaP:V^{4+}. This confirms the expected considerably larger broadening of the V^{4+} ZPLs due to the internal random strains, especially as the investigated boules of GaP:Ti and GaP:V have been grown by us in the same pulling machine with identical growing conditions.

The reduction of the Γ_7–Γ_8 spin–orbit splitting by the Jahn–Teller coupling should be also larger for V^{4+} than for Ti^{3+} (3.3 cm^{-1}). Therefore, it is reasonable to assume that the sharp line at 6968.3 cm^{-1} of GaP : V^{4+} involves the two zero-phonon lines, i.e. the Γ_7–Γ_8 splitting is certainly smaller than 5 cm^{-1}. It should be noted that the broadened ZPL of V^{4+} in InP has been interpreted in the same way [6]. The second narrow line at 23 cm^{-1} above the ZPL at 6968.3 cm^{-1} has to be assigned to a transition into an excited vibronic level of the $^2T_2$ state as it has been proposed for the second lines of Ti^{3+} in GaP and GaAs [18].

4.2. The V^{3+}/V^{4+} donor level and photo-induced recharging

By the described experiments on different *p*-type GaP:V:Zn samples, it has been proved that the V^{3+}_{Ga}/V^{4+}_{Ga} donor level is located within the gap as, on samples where the Fermi-level is pinned by this V donor level, the spectroscopic features of both V^{3+}_{Ga} and V^{4+}_{Ga} could be identified by optical absorption (internal transitions) and by EPR. The position of the V^{3+}_{Ga}/V^{4+}_{Ga} level estimated here (between 0.2 and 0.4 eV above the valence band edge) from electrical and optical experiments is in accordance with the more exact value $E_v + 0.25$ eV derived from DLTS- and DLOS-experiments on the same samples [8]. The V^{4+}/V^{5+} level, i.e. the ^2E ground state of V^{4+}_{Ga} , is located within the valence band, its position cannot be estimated from the present experiments.

The broad photo-induced absorption α_p with onset below 0.4 eV, which is proportional to the intensity of the photo-induced V^{4+} bands, can be assigned to the photoneutralization transition

$$V^{4+}_{Ga} + h\nu \to V^{3+}_{Ga} + \text{hole}_{vb}. \qquad (1)$$

This means that an electron is optically excited from the valence band into the V^{3+}/V^{4+} level creating a V^{3+} in its ground state $^3A_2$ and a hole in the valence band. The strong broad absorption in the region greater than 1.2 eV, the photo-induced increase of which is

also proportional to V^{4+}, is therefore assigned to transition (1) into the excited state $^3T_1(F)$ of V^{3+}. These assignments are confirmed by the DLOS spectrum ($\sigma_p^0(h\nu)$) of the V^{3+}/V^{4+} donor level (see figure 3 in [8]), which shows the onset of process (1) at 0.27 eV and the same spectral dependence as found in absorption.

The identification of the V^{4+} state is also supported by the photo-induced recharging experiments. From figures 12 and 13, it follows that the recharging is governed by the excitation process

$$P_{Ga}^{5+} + h\nu_{exc} \rightarrow P_{Ga}^{4+} + \text{hole}_{vb} \qquad (2)$$

followed by the capture process

$$V_{Ga}^{3+} + \text{hole}_{vb} \rightarrow V_{Ga}^{4+}. \qquad (3)$$

The photo-induced creation of P_{Ga}^{4+} and its spectral dependence as seen in figures 12 and 13 are exactly the same as investigated by Kaufmann *et al* [19] on GaP:Zn. The maximum content of phosphorous anti-site defects P_{Ga} in the investigated samples amounts to about 1–2 $\times$ 10^{16} cm^{-3}. This explains the result that the photo-induced $V^{3+} \rightarrow V^{4+}$ recharging is complete in sample PI 1535-A1 ($[P_{Ga}] > [V_{Ga}]$) whereas it can only be partly achieved in sample PI 1391-E1 ($[P_{Ga}] < [V_{Ga}]$ cf table 1).

Acknowledgments

The authors would like to thank B Clerjaud for many helpful discussions and H von Kiedrowski for the preparation of the oriented samples.

References

[1] Ulrici W, Eaves L, Friedland K, Halliday D P and Kreissl J 1986 *Mater. Sci. Forum* **10–12** 639
[2] Kreissl J and Ulrici W 1986 *Phys. Status Solidi* b **136** K133
[3] Ulrici W, Eaves L, Friedland K and Halliday D P 1987 *Phys. Status Solidi* b **141** 191
[4] Sahraoui-Tahar M, Salce B, Challis L J, Butler N, Ulrici W and Cockayne B 1989 *J. Phys.: Condens. Matter* **1** 9313
[5] Devaud B, Plot B, Lambert B, Bremond G, Guillot G, Nouailhat A, Clerjaud B and Naud C 1986 *J. Appl. Phys.* **59** 3126
[6] Clerjaud B, Côte D, Naud C, Bremond G, Guillot G and Nouailhat A 1987 *J. Crystal Growth* **83** 194
[7] Ulrici W, Kreissl J, Hayes D G, Eaves L and Friedland K 1989 *Mater. Sci. Forum* **38–41** 875
[8] Bremond G, Guillot G, Roura P and Ulrici W 1992 *Mater. Res. Soc. Symp. Proc.* **261** 229
[9] Nakib A, Houbloss S, Vasson A and Vasson A-M 1988 *J. Phys. D: Appl. Phys.* **21** 478
[10] Vasson A-M *et al* 1993 *J. Phys.: Condens. Matter* **5** 7669
[11] Casey H C, Ermanis F and Wolfstirn K B 1969 *J. Appl. Phys.* **40** 2945
[12] Neumark F G 1972 *Phys. Rev.* B **5** 408
[13] Look D C 1981 *Phys. Rev.* B **24** 5852
[14] Look D C, Chaudhuri S and Eaves L 1982 *Phys. Rev. Lett.* **49** 1728
[15] Kreissl J, Ulrici W and Gehlhoff W 1989 *Phys. Status Solidi* b **155** 597
[16] Ham F S 1972 *Electron Paramagnetic Resonance* ed S Geschwind (New York: Plenum) pp 1–119
[17] Ulrici W and Kreissl J 1988 *Proc. 5th Int. Conf. Semi-Insulating III-V Materials* ed G Grossmann and L Ledebo (Bristol: Hilger) pp 381–6
[18] Al-Shaikh A M, Qiu Q C, Roura P, Ulrici W, Clerjaud B, Bates C A and Dunn J L 1998 *J. Phys.: Condens. Matter* **10** 3367
[19] Kaufmann U, Schneider J, Woerner R, Kennedy T A and Wilsey N D 1981 *J. Phys. C: Solid State Phys.* **14** L941